Appl. Phys. B 92, 159–163 (2008)
DOI: 10.1007/s00340-008-3016-4

Applied Physics B
Lasers and Optics

D. TÜRKE
J. TEIPEL
H. GIESSEN✉

Manipulation of supercontinuum generation by stimulated cascaded four-wave mixing in tapered fibers

4. Physikalisches Institut, Universität Stuttgart, Pfaffenwaldring 57, 70550 Stuttgart, Germany

Received: 23 December 2007 / Revised version: 17 March 2008
Published online: 28 June 2008 •

ABSTRACT Tailoring supercontinuum generation is important for a number of applications. Stimulated four-wave mixing in tapered optical fibers can lead to modified initial conditions for the evolution of supercontinua. We experimentally show that synchronizing a pump pulse with an additional signal pulse induces cascaded four-wave mixing components. The spectral evolution and the interaction with the pump wavelength are investigated in detail upon increasing pump power. Furthermore it will be shown that four-wave mixing components provide the initiation for an altered shape of the spectral fiber output when soliton dynamics are involved. We finally demonstrate the altered evolution in a synchronized feedback configuration. This work can lead to a control over specific spectral components of supercontinua.

PACS 42.81.-i; 42.25.Kb

1 Introduction

After the first observation of supercontinuum (SC) generation in microstructured [1] as well as in tapered fibers [2], much effort has been spent to improve the white light spectra and to customize them to various applications such as frequency metrology [3] or nonlinear microscopy [4]. To achieve the desired characteristics of the SC, such as octave-spanning bandwidth or high output power at certain required wavelengths, the fibers have been optimized and certain processes contributing to the white light generation have been enhanced. New developments range, e.g., from increasing the bandwidth [5], over amplifying blue spectral components [6], to a broadly tunable OPO using a photonic crystal fiber [7]. Among all these achievements, an additional emphasis has been put on the investigation of single nonlinear processes, for instance four-wave mixing (FWM) [8, 9]. It has been shown [10], that nonlinear fibers with engineered dispersion and nonlinearity profiles provide an appropriate medium to achieve highly nondegenerate FWM with femtosecond pulses, as these fibers can compensate for the phase mismatch and group velocity differences which are caused by the material and waveguide dispersion. Recently, the interaction between an optical soliton and a copropagating cw-wave has been investigated in a photonic crystal fiber, generating new components by FWM [11, 12]. In general, the nonlinear behavior of photonic crystal fibers (PCF) and tapered fibers is similar. However, due to the fact that tapered fibers are easily homemade, precise engineering of a variety of waist diameters and waist lengths is achieved. We note that, to our knowledge, so far no stimulated FWM experiments have been performed in tapered fibers. In this paper we utilize the nonlinear effect of stimulated FWM to modify the SC generated in tapered fibers. Our output spectra differ significantly from the results which are commonly explained by the evolution of soliton dynamics [13]. By synchronizing a highly chirped ps signal pulse with a fs pump pulse we observe strong stimulated cascaded FWM in the normal as well as in the anomalous dispersion regime. The signal pulse is either a filtered SC which is generated in an additional tapered fiber, or it is coupled back from the actual tapered fiber itself. We show that stimulated FWM can lead to modified initial conditions for the evolution of the supercontinuum and provides the initiation for an altered shape of the spectral fiber output. By taking the phase matching condition into account, the evolving spectra are analyzed.

2 Experimental setup

In our experiments we utilized flame-drawn tapered fibers as the highly nonlinear medium. The fibers were home made in a fiber drawing rig, which gave us the opportunity to customize the fiber properties to the individual experiment. Especially the dispersion characteristics can be adjusted by choosing the appropriate waist diameter [14]. Additionally the nonlinear interaction length can be selected by varying the waist length. Figure 1 shows the experimental setup. Two tapered fibers (in the following named signal and pump fiber) were simultaneously pumped by the pulses from a Ti:sapphire laser with a repetition rate of 80 MHz and a pulse duration of 100 fs. The signal fiber was designed to offer a preferably high spectral output at the required signal wavelength. This spectral component was selected with an appropriate band pass or band edge filter. The output of the signal fiber can be delayed by a translation stage to ensure maximum temporal overlap of the signal pulse with the desired supercontinuum components generated in the pump fiber. Depending on the signal wavelength we either used an 800 nm long pass or a 900 nm short pass filter as the beam combining element. The resulting spec-

✉ Fax: +49-711-6856-5097, E-mail: giessen@physik.uni-stuttgart.de

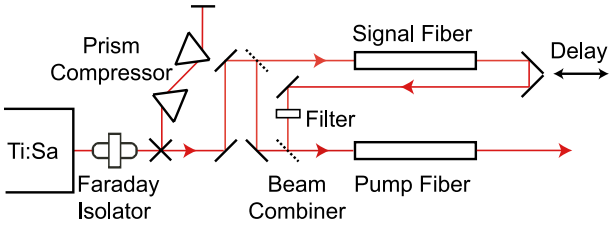

FIGURE 1 Experimental setup. The Faraday isolator which prevents back-reflections into the Laser causes a linear chirp on the pump pulses. This is compensated by a prism compressor

tra were recorded with an ANDO spectrometer (AQ6315A). For all measurements the resolution was set to 5 nm.

3 Experimental data

3.1 *FWM in the normal dispersion regime*

In order to obtain normal dispersion, a tapered fiber with 2.55 μm waist diameter, corresponding to a zero dispersion wavelength around 785 nm, has been pumped with pulses at a center wavelength of 775 nm. Figure 2 shows cartographic maps of the output spectra as a function of the Ti:sapphire input power. With increasing power the pump pulse experiences spectral broadening due to self-phase modulation (SPM) which is the main nonlinear process acting on intense pulses in the normal dispersion regime (see Fig. 2a). By synchronizing an additional signal at 902 nm (10 nm bandwidth FWHM) to the pump pulse, a FWM process is stimulated which creates an idler at the wavelength of 679 nm (see Fig. 2b). Figure 2c shows the relation between the generated idler power and the input pump power. The idler power was determined by comparing the spectral integral over the pump with the integration over the idler. With this ratio and the measured pump power the final value could be deduced. The diagram clearly demonstrates a nonlinear correlation at low powers. For high pump powers the curve turns into a linear behavior due to the spectral broadening which therefore leads to a reduction of power at the pump wavelength. For small input powers the idler component emerges at the wavelength determined by the condition of energy conservation $2\omega_{\text{pump}} = \omega_{\text{signal}} + \omega_{\text{idler}}$ (see Fig. 2b). With increasing input power signal and idler experience a blue shift. Additionally the signal starts to generate sidebands at an input power of 40 mW. This behavior can be understood by considering asymmetric cross-phase modulation (XPM) of signal and idler with the much stronger pump pulse [18]. Due to the power difference the induced chirp for the signal pulse is larger on its trailing edge. Since the trailing edge carries the blue-shifted components which have been generated by XPM, the signal pulse experiences an overall blue-shift. The same applies for the idler. A similar argument has already bee used to explain the blue shift of the non-solitonic radiation in SC generation by [19].

To gain a more detailed insight into the FWM processes we repeated the experiment with the same fiber, increasing the signal wavelength to 969 nm and the pump wavelength to 783 nm which is very close to the zero dispersion point of the fiber. Figure 3 shows a cartographic spectral map as a function of the temporal detuning of the signal pulse. This descriptive visualization has the advantage of showing the signal interacting with the different spectral components of the supercontinuum (SC) which are temporally separated due to the normal dispersion in the input pigtail of the pump fiber. As the pump wavelength is very close to the zero dispersion these components travel fastest in the fiber. The diagram shows a clear stimulated FWM process, generating an idler at 645 nm when the pump pulse temporally overlaps with the signal at a delay around 1.1 ps. The SC has a second strong component at 812 nm temporally trailing the pump wavelength by 400 fs. Delays of this amount have also been observed in the simulations of SC evolution in photonic crystal fibers by Dudley et al. [16]. Therefore the diagram shows an additional 670 nm idler at a delay around 1.5 ps. During this interaction process an asymmetric cross-phase modulation between signal and SC also takes place, causing slight spectral shifts of the signal.

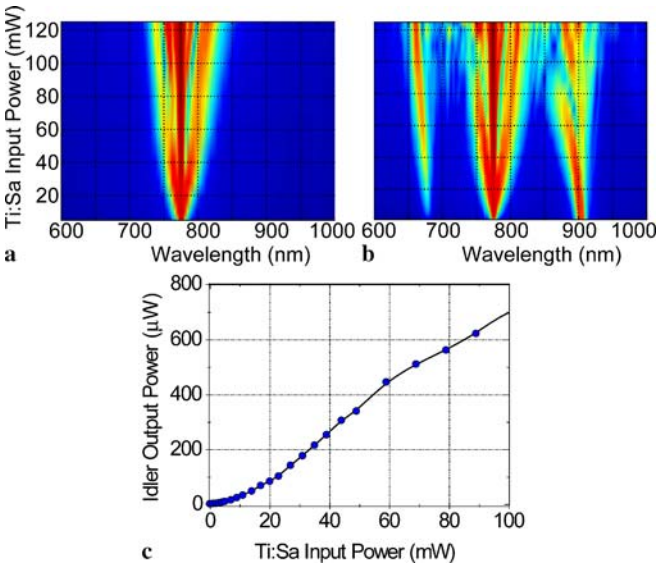

FIGURE 2 (**a**) Logarithmic spectrometer output as a function of input power. Evolution of the Ti:sapphire pulse at 775 nm in a tapered fiber with 2.55 μm waist diameter and 90 mm waist length. The throughput of the fiber was 35%. (**b**) Evolution of the Ti:sapphire pulse synchronized with a signal pulse at 902 nm and 1.6 mW input/0.65 mW output power. (**c**) Correlation between the generated idler output power and the input pump power while the signal power is kept constant

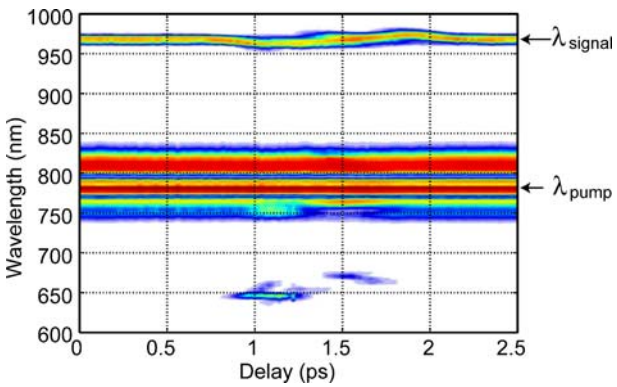

FIGURE 3 Cartographical spectral map as a function of temporal signal detuning for an input pump power of 50 mW at 783 nm for a tapered fiber of 2.55 μm waist diameter and 90 mm waist length. The throughput was 52%. The signal duration was estimated to be 240 fs based on measured XFROG including the normal dispersion in the output pigtail (cf. [20]). The signal input power was 1.6 mW at a wavelength of 969 nm (14 nm bandwidth FWHM) and the output power was 0.45 mW

3.2 *FWM and reduced soliton dynamics in the anomalous dispersion regime*

To investigate the interaction between the FWM processes and the subsequent soliton dynamics, experiments with pump pulses in the anomalous dispersion regime were performed. Figure 4 shows the results for a measurement at low input powers. The utilized fiber had a waist diameter of 2.0 μm, corresponding to a zero dispersion wavelength of 710 nm. When signal (690 nm) and pump (802 nm) are temporally detuned (see Fig. 4a) we see an increased SPM broadening of the pump pulse with increasing power. The synchronization (see Fig. 4b) allows a stimulation of two competing FWM processes. When the pump input is below 7 mW, the signal pulse is the more intense one and acts as the pump for a FWM process, creating one photon at 802 nm and one at 605 nm. This is stimulated by the pump wavelength. We see a splitting of the signal pulse due to XPM. This splitting starts from a symmetric behavior when signal and pump have similar intensities and evolves into an asymmetric behavior when the pump pulse becomes more intense. When the pump pulse exceeds the signal intensity the expected stimulated FWM process starts generating an idler at 957 nm. With further increase of the pump power these cascaded FWM processes can be enhanced. Figure 5 shows the cartographical spectral map as a function of temporal signal detuning for such a case. Five cascading processes are stimulated, covering a spectral range down to 550 nm. At the same time the intensity of the pump wavelength is characteristically and substantially reduced which is well documented in the figure. The 45 nm bandwidth signal has gained a huge normal dispersion in the output pigtail of the fiber where it has been generated. Therefore the chirped signal components are temporally overlapping with the pump pulse for increasing detuning. This leads to the curved signal trace which continues in the FWM cascades. Consequently the idler in the infrared, corresponding to the initial signal has a mirrored curvature. The behavior changes slightly when the signal wavelength is placed above the pump which is illustrated in Fig. 6a. This figure shows a cartographic spectral map as a function of temporal signal detuning for the same fiber already utilized in Fig. 5. We see again the cascaded FWM which is less pronounced. To enhance the number of cascades and therefore the width of the spectrum, a higher nonlinearity of the fiber is essential. Figure 6b shows a comparison of the FWM cascades building up in three different fibers, all having 15 mm waist length but different waist diameters. We see that the number of cascades increases for thinner waist diameters as this corresponds to a higher nonlinearity. For the 1.7 μm waist the number of cascades is 6 and the spectrum spans over the broadest region down to 470 nm.

To visualize the dramatic effect of the FWM on the soliton dynamics, we performed an experiment with a longer fiber and therefore a higher interaction length (see Fig. 7). The infrared part of the spectrum at high power shows self-frequency shifted solitons, and the blue part is the corresponding non-solitonic radiation. The spectral shapes together with their temporal equivalents are beautifully shown in the review by Dudley et al. [21]. When the signal and a component of the SC are now temporally synchronized, the spectral evolution changes substantially. At low input powers an idler component is generated at the energy-conserving wavelength of 707 nm. Driven by this initiation with increasing input power the spectrum evolves into the symmetric shape shown in Fig. 7b with signal and idler dominating the spectrum. Consequently the peak around the pump wavelength is simultaneously reduced. The overall shape does not show the solitonic behavior which we can see in Fig. 7a. Thus the soliton dynamics are completely suppressed. The outward shift of the signal and idler component can be explained by taking

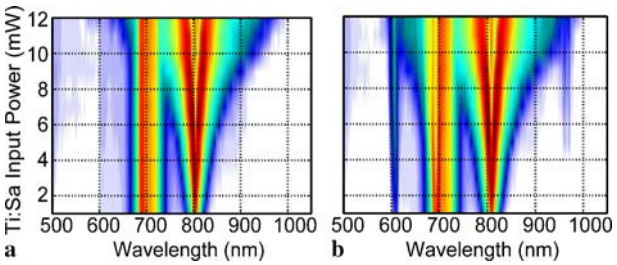

FIGURE 4 Logarithmic spectrometer output as a function of input power. (**a**) Evolution of the Ti:sapphire pulse at 802 nm in a tapered fiber with 2.0 μm waist diameter and 90 mm waist length when signal and pump pulse are temporally detuned. The throughput of the fiber was 50%. (**b**) Evolution of the Ti:sapphire pulse synchronized with a 37 nm (FWHM) bandwidth signal pulse at 690 nm. The signal input/output power was 8.9/3.4 mW

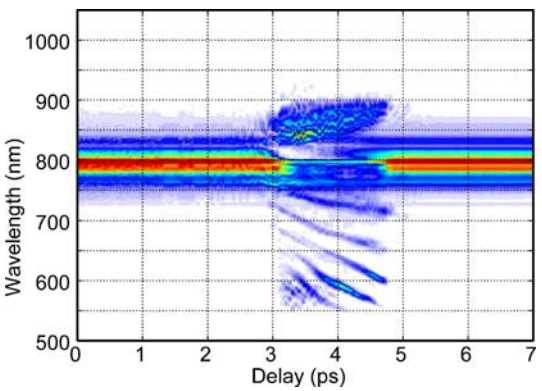

FIGURE 5 Cartographical spectral map as a function of temporal signal detuning for an input pump power of 175 mW at 800 nm for a tapered fiber of 1.9 μm waist diameter and 15 mm waist length. The throughput was 69%. The signal input power was 4.0 mW at a wavelength of 735 nm (45 nm bandwidth FWHM). The signal output power was 2.4 mW

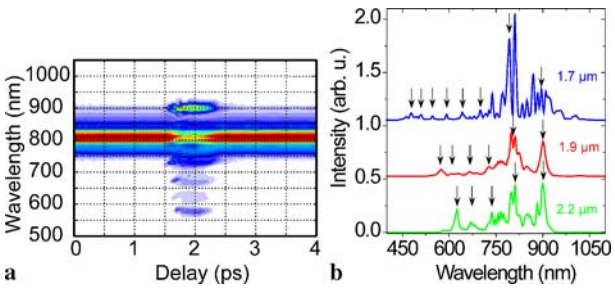

FIGURE 6 Output spectra of tapered fibers with 15 mm waist length, an input pump power of 185 mW, and 814 nm pump wavelength. The signal wavelength was 900 nm (10 nm bandwidth FWHM). (**a**) Cartographical spectral map as a function of temporal signal detuning for a 1.9 μm fiber. The throughput was 65%. The signal input power was 1.2 mW and the output power was 0.40 mW. (**b**) Synchronized spectra of fibers with different waist diameters

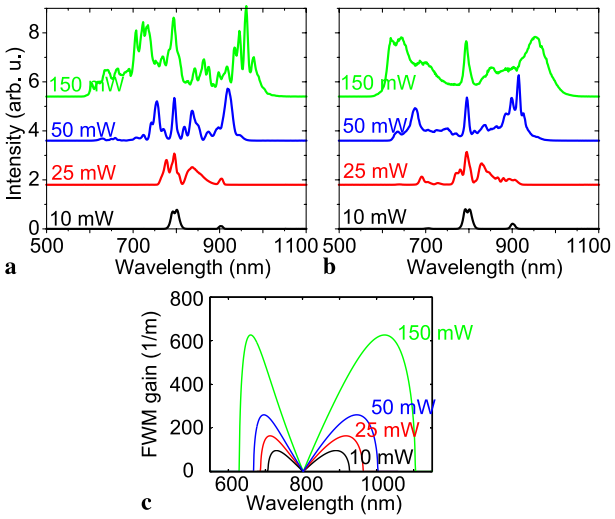

FIGURE 7 Linear spectrometer output for different input powers. The tapered fiber had a waist diameter of 2.55 µm, a waist length of 90 mm, and a throughput of 61%. The signal input power was 1.4 mW at a wavelength of 900 nm (10 nm bandwidth FWHM). The signal output power was 0.4 mW. (**a**) Signal pulse and SC are temporally detuned. (**b**) Signal pulse and SC component at 792 nm are temporally synchronized. (**c**) Corresponding FWM gain resulting from the phase-matching condition

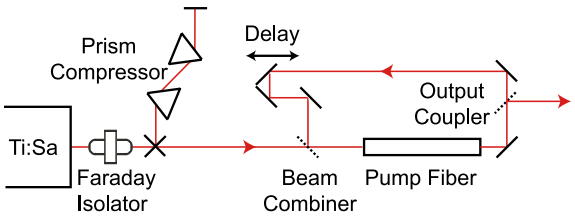

FIGURE 8 Experimental setup for the feedback configuration. Only a single fiber is used to generate the signal and the SC

the phase-matching condition for degenerate FWM ($2\gamma P_0 + 2k_0 + k_1 + k_2 = 0$) into account [15]. Figure 7c shows the simulated FWM gain for the experimental situation of Fig. 7b. With higher input power the gain maxima increase and show an analogous outward shift. We assume, that the pump pulse duration does not change much along the waist as we are close to the zero-dispersion wavelength. Therefore, we assume the FWM gain spectrum remains approximately the same along the waist.

3.3 *Stimulated cascaded FWM in a feedback configuration*

To simplify the setup, we now utilize only a single fiber to generate the signal and the SC (see Fig. 8). The SC was fed back into the pump fiber to serve as the signal. Like in the previous experiments the synchronization between the signal pulse and the subsequent pump pulse was achieved by an optical delay. As the beam combining element we used an 800 nm long pass filter. Therefore, only components below 800 nm contribute to the synchronization with the pump pulse. A glass plate served as the output coupler. Figure 9 depicts the output spectra of such a synchronized and detuned feedback configuration. In comparison to Fig. 5 we see a very similar cascading process, generating four detached spectral peaks at wavelengths which can only be obtained by

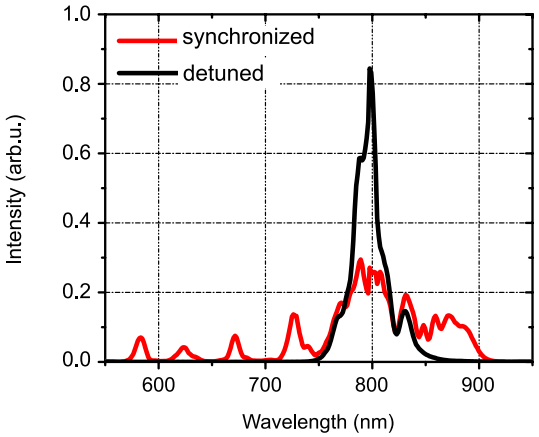

FIGURE 9 Linear spectrometer output in the single fiber feedback configuration. The tapered fiber had a wait diameter of 1.9 µm, a waist length of 15 mm. The input pump power was 185 mW. The throughput was 65%. The beam combining element was a 800 nm long pass filter

enhanced non-solitonic radiation in a regular SC generation scheme. These signals were previously interpreted as tapered fiber OPO effects [17]. The depletion of the pump peak by a factor of three at 800 nm in the synchronized case is nicely visible.

4 Conclusions

We have shown that FWM can be stimulated by synchronizing a pump pulse with an additional signal pulse in a tapered fiber. At higher pump intensities this FWM can be enhanced and generates a wide range of up to six cascaded idler components. When pumping in the anomalous dispersion regime the regular soliton dynamics can be suppressed and replaced by strong FWM as the dominant nonlinear process. The temporal synchronization of a signal to the pump alters the initial conditions for SC evolution, leading to an exceptional spectral shape. The phase-matching condition thereby provides an indication in which way the overall SC will evolve. A simplified setup which uses only one tapered fiber and a synchronized feedback yielded similar results. Our work shows a way of influencing supercontinuum generation in a controlled way, which could be useful in applications such as nonlinear microscopy and spectroscopy.

ACKNOWLEDGEMENTS The authors are grateful for financial support by DFG (FOR 557) and BMBF (13N8340).

REFERENCES

1 J.K. Ranka, R.S. Windeler, A.J. Stentz, Opt. Lett. **25**, 25 (2000)
2 T.A. Birks, W.J. Wadsworth, P.S.J. Russell, Opt. Lett. **25**, 1415 (2000)
3 R. Holzwarth, T. Udem, T.W. Hansch, J.C. Knight, W.J. Wadsworth, P.S.J. Russell, Phys. Rev. Lett. **85**, 2264 (2000)
4 T. Betz, J. Teipel, D. Koch, W. Hartig, J. Guck, J. Käs, H. Giessen, J. Biomed. Opt. **10**, 054009-1 (2005)
5 C.M.B. Cordeiro, W.J. Wadsworth, T.A. Birks, P.S.J. Russell, Opt. Lett. **30**, 1980 (2005)
6 I. Cristiani, R. Tediosi, L. Tartara, V. Degiorgio, Opt. Express **12**, 124 (2004)
7 Y. Deng, Q. Lin, F. Lu, G.P. Agrawal, W.H. Knox, Opt. Lett. **30**, 1234 (2005)

8 J.E. Sharping, M. Fiorentino, A. Coker, P. Kumar, R.S. Windeler, Opt. Lett. **26**, 1048 (2001)
9 S. Coen, A.H.L. Chau, R. Leonhardt, J.D. Harvey, J.C. Knight, W.J. Wadsworth, P.S.J. Russell, J. Opt. Soc. Am. B **19**, 753 (2002)
10 K.S. Abedin, J.T. Gopinath, E.P. Ippen, C.E. Kerbage, R.S. Windeler, B.J. Eggleton, Appl. Phys. Lett. **81**, 1384 (2002)
11 A. Efimov, A.V. Yulin, D.V. Skryabin, J.C. Knight, N. Joly, F.G. Omenetto, A.J. Taylor, P.S.J. Russell, Phys. Rev. Lett. **95**, 213902-1 (2005)
12 C. Cheng, X. Wang, Z. Fang, B. Shen, Appl. Phys. B **80**, 291 (2005)
13 A.V. Husakou J. Hermann, J. Opt. Soc. Am. B **19**, 2171 (2002)
14 J. Teipel, K. Franke, D. Türke, F. Warken, D. Meiser, M. Leuschner, H. Giessen, Appl. Phys. B **77**, 245 (2003)
15 G.P. Agrawal, *Nonlinear Fiber Optics*, 3rd edn. (Academic, San Diego, CA, 2001)
16 J.M. Dudley, X. Gu, L. Xu, M. Kimmel, E. Zeek, P. O'Shea, R. Trebino, S. Coen, R.S. Windeler, Opt. Express **10**, 1215 (2002)
17 H. Giessen, J. Teipel, CLEO/QELS Technical Digest on CD-ROM (Opt. Soc. Amer., Washington, DC, 2003), CMO3
18 M.N. Islam, L.F. Mollenauer, R.H. Stolen, J.R. Simpson, H.T. Shang, Opt. Lett. **12**, 625 (1987)
19 T. Schreiber, T.V. Andersen, D. Schimpf, J. Limpert, A. Tünnermann, Opt. Express **13**, 9558 (2005)
20 D. Türke, W. Wohlleben, J. Teipel, M. Motzkus, B. Kibler, J. Dudley, H. Giessen, Appl. Phys. B **83**, 37 (2006)
21 J.M. Dudley, G. Genty, S. Coen, Rev. Mod. Phys. **78**, 1135 (2006)